RESEARCH PAPER

One-step preparation of antimicrobial silver nanoparticles in polymer matrix

O. Lyutakov · Y. Kalachyova · A. Solovyev · S. Vytykacova · J. Svanda · J. Siegel · P. Ulbrich · V. Svorcik

Abstract Simple one-step procedure for in situ preparation of silver nanoparticles (AgNPs) in the polymer thin films is described. Nanoparticles (NPs) were prepared by reaction of *N*-methyl pyrrolidone with silver salt in semi-dry polymer film and characterized by transmission electron microscopy, XPS, and UV–Vis spectroscopy techniques. Direct synthesis of NPs in polymer has several advantages; even though it avoids time-consuming NPs mixing with polymer matrix, uniform silver distribution in polymethylmethacrylate (PMMA) films is achieved without necessity of additional stabilization. The influence of the silver concentration, reaction temperature and time on reaction conversion rate, and the size and size-distribution of the AgNPs was investigated. Polymer films doped with AgNPs were tested for their antibacterial activity on Gram-negative bacteria. Antimicrobial properties of AgNPs/PMMA films were found to be depended on NPs concentration, their size and distribution. Proposed one-step synthesis of functional polymer containing AgNPs is environmentally friendly, experimentally simple and extremely quick. It opens up new possibilities in development of antimicrobial coatings with medical and sanitation applications.

Keywords Polymer · Silver nanoparticles · TEM, XPS and UV–Vis characterization · Antimicrobial test · Health effects

O. Lyutakov (✉) · Y. Kalachyova · J. Svanda · J. Siegel · V. Svorcik
Department of Solid State Engineering, Institute of Chemical Technology, 166 28 Prague, Czech Republic
e-mail: lyutakoo@vscht.cz

A. Solovyev
Institute of Chemical Process Fundamentals of the ASCR, 165 02 Prague, Czech Republic

S. Vytykacova
Department of Glass and Ceramics, Institute of Chemical Technology, 166 28 Prague, Czech Republic

P. Ulbrich
Department of Biochemistry and Microbiology, Institute of Chemical Technology, 166 28 Prague, Czech Republic

Introduction

Silver is well-known antimicrobial agent. Its activity against bacteria is especially pronounced in the nanoparticle form silver nanoparticles (AgNPs; Rai et al. 2009; Kumar and Münstedt 2005). Materials doped with AgNPs may preserve their bactericidal activity over a long-time period (Melaiye 2005). Combination of polymer with AgNPs provides excellent material for perfect antimicrobial coatings (Jain and Pradeep 2005; Lyutakov 2014). The general method of polymer/nanoparticles (NPs) nanocomposite preparation consists in the dispersion of formerly prepared colloidal nanoparticles (AgNPs) in the polymer solution (Lim and Ast 2000). Preparation of

NPs also includes careful choice of solvent medium, reducing agent, and materials for the stabilization of the AgNPs (Raveendran et al. 2003; Fanta et al. 2013; Shameli 2012). Application of the same compound serving as a silver reducing agent as well as dispersing and stabilizing agent of the resulting AgNPs can simplify NPs preparation (Fei et al. 2013; Chudasama et al. 2010). The most common synthesis of AgNPs is the chemical reduction of a silver salt solution by a reducing agent (Sioss and Keating 2005). In this case, the size, distribution of AgNPs, and their antimicrobial activity are a function of reductant—strong reductant leads to creation of small monodispersed AgNPs, while weaker reductant to a slower reduction rate resulting in broader size distribution (Marambio-Jones and Hoek 2010). However, reducing agents may very often be associated with environmental toxicity or biological hazards, preventing application of AgNPs in medicine. Moreover, AgNPs synthesized by those methods easily aggregate, which worsens processability, deteriorates useful AgNPs properties, and decreases their antibacterial properties. Alternative method of AgNPs preparation based on so-called green chemistry was proposed too (Sharma et al. 2009). Some of the most promising ways of green AgNPs synthesis utilizes N-methyl pyrrolidone (NMP) or polyvinylpyrrolidon (PVP). Because of their low toxicity and acceptable biocompatibility, NMP and PVP are considered as suitable candidates for medical application. NMP-based synthesis of AgNPs allows their precise shape and size control. AgNPs between 50 and 350 nm in size were synthesized by heating of aqueous solution of $AgNO_3$ and PVP Washio (2006). NMP-based synthesis of triangular AgNPs with controllable size was reported in Jeon et al. (2009). Additionally, poly(vinyl pyrrolidone) can be used as both a steric stabilizer and a reducing agent for controllable growth of silver triangular nanoplates (Washio et al. 2006).

During the process of mixing with polymer, AgNPs tend to aggregate and lose their antimicrobial properties (Qu 2014). This phenomenon becomes more pronounced due to high viscosity of molten polymers or polymers solution. Additionally, the presence of stabilizers can reduce antimicrobial activity compared to pure silver NPs (Phu 2014; Burkowska-But et al. 2014). To overcome this problem, two approaches have been introduced over the past few years: polymerization of monomer in the presence of AgNPs and preparation of NPs directly in polymer matrix or in polymer solution (Vukoje 2014; Yoksan and Chirachanchai 2009). Application of in situ synthesis of NPs in polymer matrix can produce uniform distribution and allows precise control of NPs morphology too. Simple organic polymers and more sophisticated systems, including biological macromolecules, block co-polymers, dendrimers, and gels can provide well-defined distribution and morphologies of NPs (Behrens et al. 2006; Naik 2004; Jewrajka and Chatterjee 2006; Grubbs 2005; Sun 2003; Mohan 2006; Jin and Yuan 2005).

In this paper, we propose novel experimentally simple preparation technique of polymer–AgNPs composite which effectively prevents AgNPs aggregation. AgNPs were synthesized in the polymer matrix by reduction of silver nitrate with NMP in one-step procedure after polymer deposition.

Experimental

Materials

Anhydrous N-methyl-2-pyrrolidone (NMP, purity 99.5 %, supplied by Sigma Aldrich), and silver nitrate ($AgNO_3$, purity 99.9999 %, supplied by Sigma Aldrich), were used as received. (PMMA, $M_w = 1,459,000$) of optical purity was supplied from Goodfellow. Mueller–Hinton broth (MHB; Oxoid, CM0405) and Mueller–Hinton agar (Oxoid, CM0337) were prepared as described by producer and sterilized in autoclave.

Nanoparticles preparation

Different amounts of $AgNO_3$ were dissolved in N-methyl pyrrolidone and mixed with 7 % solution of PMMA in chloroform. Weighed portion of silver nitrate was chosen to obtain 1, 3, 5, 7, and 10 % silver concentration in the dried PMMA. Then, thin films were rapidly deposited by spin-coating (1000 rpm, 30 s) onto hot plate (at 50, 75, 100, 150, 200 and 250 °C) and further heated until appearance of uniform yellow coloration.

Characterization

The size and distribution of AgNPs in PMMA films were determined by transmission electron microscopy (TEM) on JEOL JEM-1010 instrument operated at 80 kV. Polymer films were separated from glass substrate and for TEM measurements, cca 100-nm-thick plates were cut by ultra-cutter. Additionally, UV–Vis absorption spectroscopy was used to estimate size distribution of NPs using Mie theory (Mie 1908; Manikandan et al. 2003). Refraction index of PMMA necessary for the calculation was taken from our previous work (Lyutakov 2008; Svorcik et al. 2008). Conversion rate of Ag^+ into AgNPs was determined by XPS spectroscopy on Omicron Nanotechnology ESCAProbeP spectrometer. The analyzed area had dimensions of 2×3 mm^2. Optical spectroscopy was used to indicate AgNPs creation and releasing during film soaking. UV–Vis absorption spectra were measured using Spectrometer Lambda 25 (Perkin-Elmer). AFM technique in tapping mode with Digital Instruments CP II set-up was used for characterization of the surface morphology.

Antimicrobial effect

Antimicrobial tests were performed by sample soaking and measurement of antimicrobial properties of the extracts. Plate with film (1 cm^2) was incubated in a dH$_2$O (3 ml) in a 12-well plate (Corning) for 1, 3, 6, and 12 h in orbital shaker (100 rpm) Unimax 1000 (Heidolph) at RT within 1, 3, 6, and 12 h. Pristine PMMA films prepared from mixed chloroform/NMP solution without AgNPs were used as control samples. Fresh samples and samples previously soaked in dH$_2$O (50 ml) were used to evaluate antimicrobial activity.

The antimicrobial effect of AgNPs was carried out using a gram-negative *Escherichia coli*. One colony was inoculated with 50 ml of MHB medium and incubated in orbital shaker Unimax 1000 (Heidolph) at 37 °C, 200 rpm to OD$_{600}$ 0.3. Extracts (50 μl), MHB (220 μl) and cultivated cells (30 μl) were added to each well of 96-well microplate (Corning), 50 μl dH$_2$O instead extracts was added as control. The cells growth was monitored by changing of the transmitted light absorption at 600 nm on microplate spectrophotometer SPECTROstar Omega (BMG Labtech, measurement of OD$_{600}$ every 30 min at 37 °C, before each measurement the double orbital shaking was applied at 200 rpm for 20 s).

Result and discussion

AgNPs synthesis

Scheme of preparation of AgNPs/PMMA composite is shown in the Fig. 1. The spin-coated films containing PMMA and AgNO$_3$ were hold for a time ensuring full chloroform evaporation (Fig. 1b). Then semi-dry films were rapidly placed at hot plate, where reduction of silver occurred in several sec (Fig. 1c). Residual amount of NMP and byproducts (BP) were simultaneously evaporated. According to (Marambio-Jones and Hoek 2010), main BP are 5-hydroxy-*N*-methyl pyrrolidone, *N*-methyl succinimide, and nitrate derivatives. During preparation procedure, yellowing of the samples was observed (see Fig. 5). Uniform yellow coloring indicates UV–Vis absorption band near 450 nm which is typical for plasmon resonance in AgNPs. In proposed reaction scheme (Marambio-Jones and Hoek 2010), NMP is oxidized in the presence of oxygen and at elevated temperature forms peroxide species transforming NMP to 5-hydroxy-*N*-methyl-2-pyrrolidone which acts as a reducing agent. As a result, *N*-methyl succinimide and AgNPs are produced. Additionally, it should be noted that in the case of our NMP plays a dual role: (i) acts as a diffusion promoter and (ii) as a reducing agent. NMP exhibits high penetrability and diffusion coefficient in amorphous polymer (Zellers and Sulewski 1993; Jou et al. 1992) and thus it can enhance silver diffusion into polymer matrix (Akhter and Barry 1985). NMP is also known to stabilize NPs and prevent their aggregation (Giordani et al. 2006; Frolov et al. 2012). Attempts to repeat the sample preparation using THF, DMSO, or DMFA as solvent for AgNO$_3$ led to significantly lower intensity of staining or to samples degradation (blackening) depending on the applied temperature.

Figure 2 shows AgNPs distribution in PMMA films measured by TEM. Corner inset in Fig. 2 illustrates the shape of individual AgNPs. AgNPs shape is rather different from spherical one. NPs are in the form of irregular polygons, with sharp edges. Similar shape was observed for AgNPs synthesized by Ag^+ reaction with PVP or NMP (Marambio-Jones and Hoek 2010;
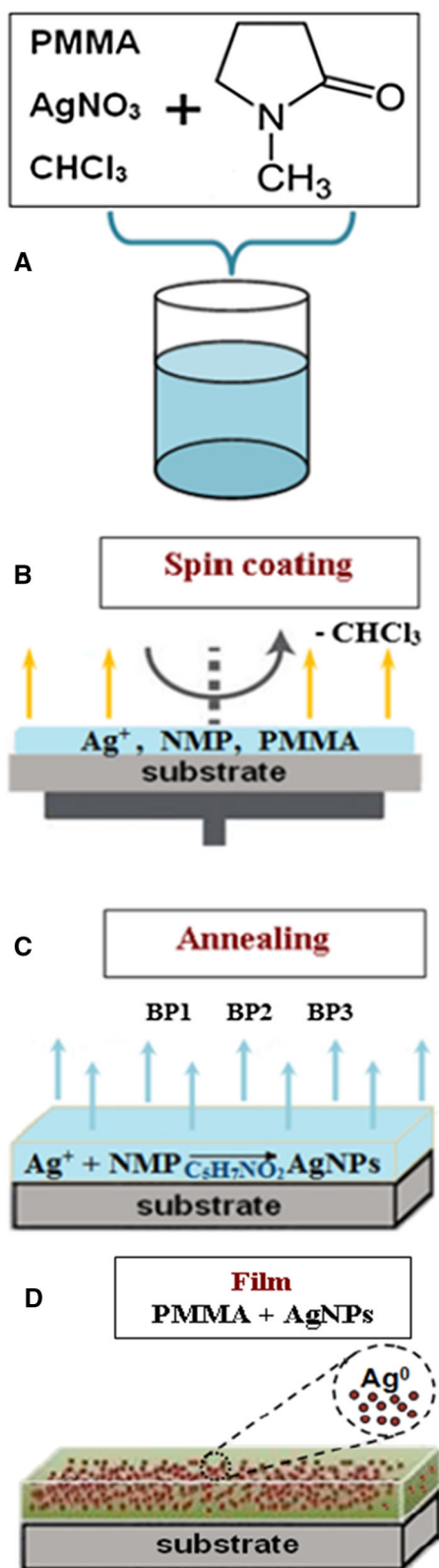
Washio et al. 2006; Jeon et al. 2009). It should be noted that NPs with sharp edges are more biologically active than spherical ones. So that the irregular form of prepared NPs can contribute to AgNPs/PMMA films antimicrobial properties. It is well known that silver segregation in polymer matrix can lead to significant loss of advantageous nanocomposite optical or antimicrobial properties Cheviron et al. (2014). By proper choice of polymer and preparation condition, silver aggregation can be prevented (Damm and Munstedt 2008). Recent research efforts have been directed toward exploiting the in situ synthesis of metal NPs inside of polymeric materials (Aymonier et al. 2002; Ho et al. 2004). In situ formation of AgNPs with good uniformity and distribution was reported, for example, in photo-crosslinking methacrylate polymers (Cheng et al. 2011) and co-polymers (Mohan 2006). In the last case, uniformity of NPs dispersion was significantly affected by co-polymer composition (Mohan 2006). Another approach consists in immobilization of silver ions followed by their reduction. This process requires the presence of charged group on polymer surface or in bulk (Son et al. 2006; Kong and Jang 2008; Dallas et al. 2011). In usual case, uniformity of NPs distribution is enhanced through silver restriction by chemical or physical interaction or by polymer matrix freezing. From comparison of the present TEM images with those available from literature, it can be concluded that the AgNPs distribution is more or less acceptable (Mohan 2006; Cheviron et al 2014; Damm and Munstedt 2008; Aymonier et al. 2002; Ho et al. 2004; Cheng et al. 2011; Son et al. 2006; Kong and Jang 2008; Dallas et al. 2011). Individual AgNPs aggregates are visible, but mostly well-separated NPs are seen. So, it may be concluded that an appropriate quality of AgNPs distribution was achieved mainly thanks to two stages of solvent evaporation (see Fig. 2). First, dichloroethane was evaporated during spin-coating procedure. Formation of AgNPs was performed in semi-
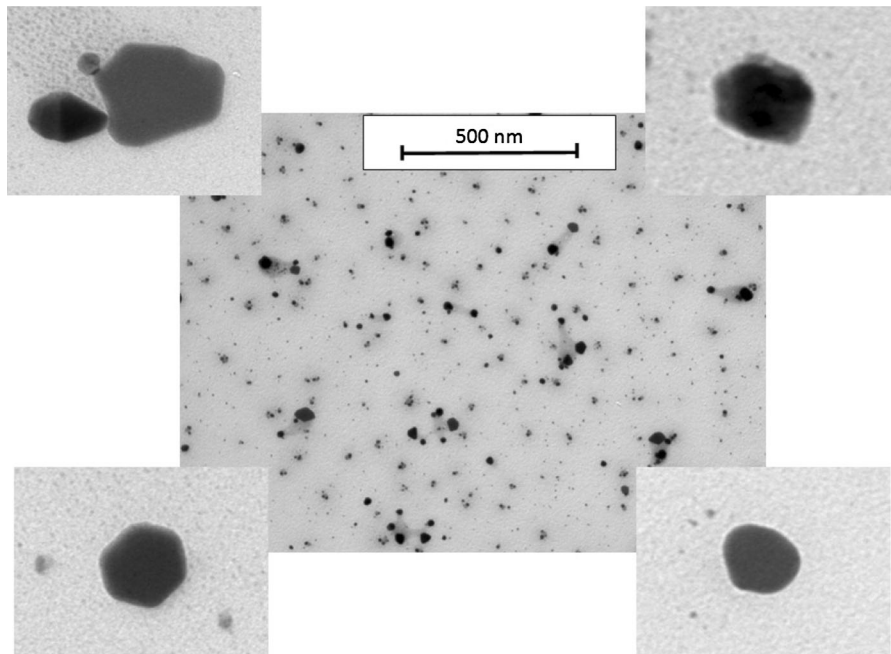
Fig. 2 TEM image of AgNPs distribution in PMMA films; 20×20 µm corner *insets* show the shape of individual particles

dried polymer films, containing only NMP. At these conditions, diffusion of Ag ions occurs, but NPs are entrapped. As a result, aggregation of AgNPs does not occur.

For the determination of the conversion rate of Ag^+ into AgNPs, XPS technique was applied. Result of
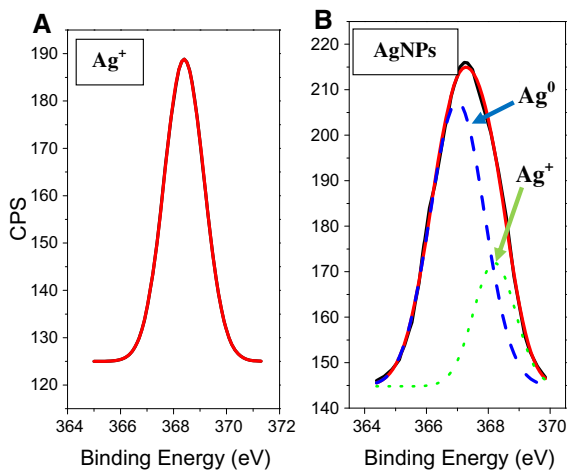

Fig. 3 XPS spectra from reference sample polymer films doped with Ag^+ (**a**) and from AgNPs (**b**). Gaussian approximation was used for fitting of Ag^+ and Ag^0 peaks. Peak parameters are presented in the Table 1

typical XPS measurement is presented in Fig. 3. In usual case, it is difficult to separate Ag^+ and Ag^0 peaks because they are close to each other. Therefore "reference" sample in which the reduction of silver was not carried out was also measured (Fig. 3a). Reference sample was prepared through substitution of NMP by THF and centrifugation for 30 min without sample heating. Conservation of Ag^+ state was controlled by film transparency and absence of yellow coloring. XPS spectrum from sample with AgNPs is shown in Fig. 3b. XPS spectra were evaluated by fitting in Gaussian approximation and the resulting peaks parameters are given in the Table 1. The spectrum from Ag^+/PMMA film can be fitted with one peak but the spectrum from AgNPs/PMMA film is a superposition of two peaks, attributed to reduced and unreacted silver. Peak maximum of Ag^+ is lying at 368.44 eV in the case of Ag^+/PMMA film. For AgNPs/PMMA films, the same maximum is shifted to 368.2. The shift can be attributed to different film chargings. Peak corresponding to Ag^0 was found only in the case of AgNPs/PMMA film and its maximum is at 367 eV. In both cases peaks, width (FWHM) is below 2 eV, which value is typical for element in the same valence state. Since the area of evaluated peaks is proportional to concentration, we were able to

Table 1 Data from evaluation of XPS spectra (from Fig. 3) for Ag^+/PMMA and AgNPs/PMMA samples

Sample	Ag	Peak area	Peak position (eV)	Peak FWHM (eV)
Ag^+/PMMA	Ag^+	135 ± 3	368.4 ± 0.1	1.7 ± 0.1
AgNPs/PMMA	Ag^0	148 ± 9	367.1 ± 0.1	1.8 ± 0.1
	Ag^+	37 ± 8	368.2 ± 0.1	1.4 ± 0.1

estimate the conversion rate of reduced silver at different experimental conditions. Table 2 gives the reaction time and conversion rate of silver. Reaction time was estimated from absorption measurements as the time after which the film ceased to change color. Reaction time was found to be affected only by applied temperature and to be independent on silver concentration. The reaction proceeds for several hours at low temperatures and for few seconds at high temperatures. Conversion rate of silver, however, was found to be influenced by both temperature and silver concentration. Depending on these parameters, silver ions conversion can be varied from 20 to 95 %. For low silver concentrations, the reactivity is higher at low temperatures but for high concentrations the reactivity is higher at higher temperatures. In the case of medium concentration, some temperature optimum can be found.

Figure 4 shows the average size and distribution of AgNPs as a function of both silver concentration and applied temperature. The data were obtained from the fit of the measured data by Gaussian curve. As can be seen from Fig. 4a, the AgNPs size depends on the silver concentration and applied temperature. Since the temperature determines reaction time (see Table 2) it can be concluded that both parameters influence the size of AgNPs. As a function of the applied temperature, the AgNPs radius varies in

several nanometers range, but all curves exhibit distinctive maximum. With increasing silver concentration, position of maximum is shifted to lower temperature. Figure 4b shows the width of the NPs distribution calculated from FWHM of the Gaussian approximation of AgNPs (upper x-axis shows the logarithm of the reaction time). Like in the previous case, silver concentration, reaction time (or temperature) influence the NPs distribution. For lower silver concentrations, wider distributions were obtained at a lower temperature. Difference becomes less pronounced with increasing Ag concentration. For 10 % Ag concentration, the narrowest distribution was obtained at the 50 °C temperature.

In works on silver reduction by NMP, the attention has mainly been focused on applications for surface Raman enhancement (Kim 2013) but here we shall address another important silver property—its antimicrobial properties (Kong and Jang 2008). First, release of silver from AgNPs/PMMA films was determined by measurements of UV–Vis absorption spectra (see Fig. 5). Samples were soaked in dH_2O and changes in their UV–Vis absorption spectra were followed. Surface plasmon absorption peak at 350–550 nm wavelengths range indicates the presence of AgNPs. Decrease of the absorption peak intensity (Fig. 5) indicates gradual elution of AgNPs during films soaking. The elution takes place only during first 24 h of soaking. Further films soaking do not affect AgNPs content in the film. It appears that only a part of AgNPs can be released and another part is firmly incorporated in polymer matrix. Surface morphologies of polymer films before and after film soaking are shown in Fig. 6. Apparent deviation from a flat surface can be attributed to the presence of AgNPs. After film soaking, surface morphology is dramatically changed, namely instead of AgNPs holes appear. It can therefore be concluded that AgNPs are released mostly from near surface region of polymer.

For antimicrobial tests, *E. coli* able to create biofilms was chosen as typical model for pathogen

Table 2 The reaction time (min) and silver conversion rate (%) in dependence on applied temperature (°C)

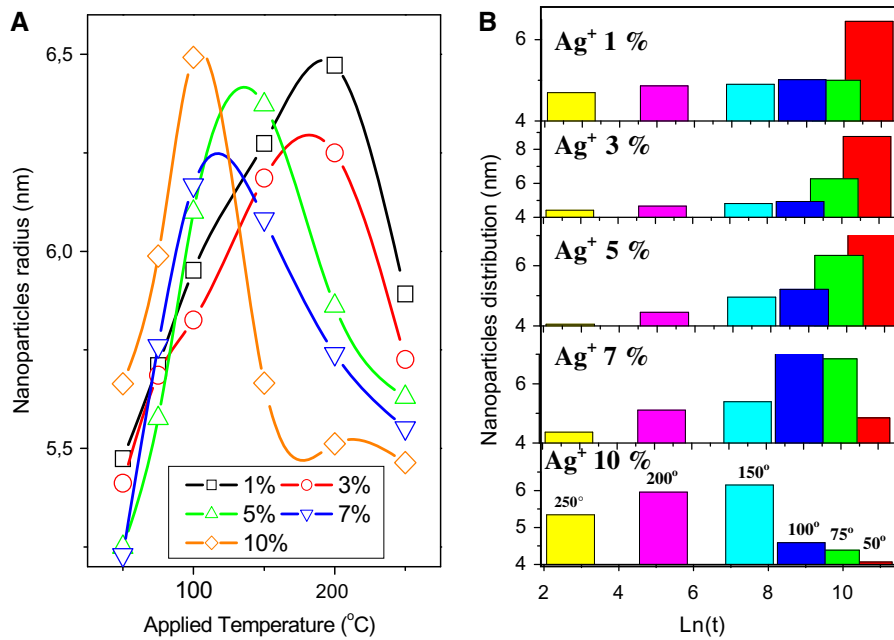| Ag^+ concentration (%)	Applied temperature (°C)					
	50	75	100	150	200	250
	Reaction time (min)					
	720	300	120	30	3	0.15
1	75	61	48	36	31	36
3	36	42	80	94	68	60
5	18	31	72	74	60	54
7	15	46	50	58	58	63
10	18	67	70	74	78	82

Fig. 4 AgNPs size (**a**) and size distribution (**b**) in dependence on the applied temperature and processing time (*t*)
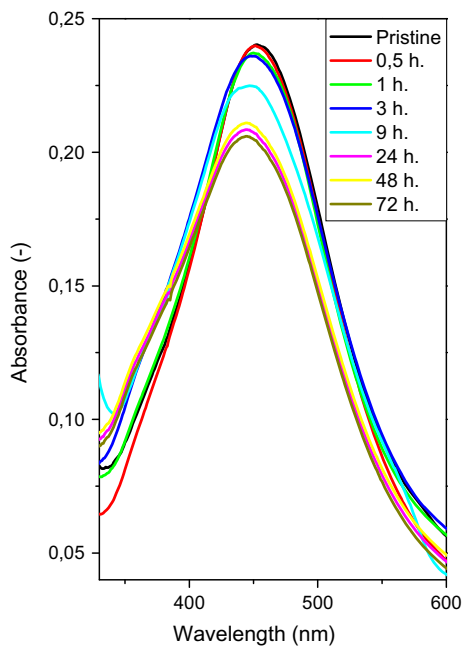

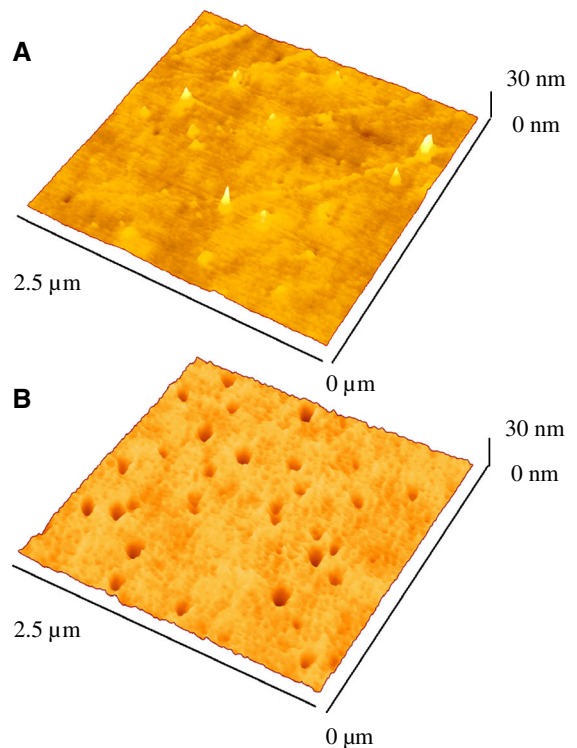**Fig. 5** UV–Vis absorption spectra of AgNPs/PMMA films as prepared and after different soaking times

Fig. 6 AFM images of AgNPs/PMMA films before (**a**) and after (**b**) soaking for 24 h

bacteria. AgNPs/PMMA films were soaked in distilled water and extracted solution was mixed with nutrient solution and bacteria cells were added. Figure 7 represents the antimicrobial activity of prepared films. Figure 7a shows evolution of optical density (OD) of bacteria suspension (different concentrations of silver, constant temperature of 100 °C). The OD is dimensionless unit representing the absorbance of material measured at 630 nm wavelength and is proportional to the number of bacteria cells. Bacteria growth leads to an increase of the OD and a decrease of the OD indicate silver inhibition effect. In the case of 10 % Ag concentration antimicrobial activity is apparent and undeniable. The quite different situation is observed in the case of lower Ag concentrations. There are no significant differences between control samples and samples containing 7 % or less of silver. In these cases bacteria, growth starts as in control sample and after a certain time the growth curves exhibit only slight deviation from the control curve. So, it can be concluded that only weak antimicrobial activity appears if the samples contain "low" silver concentration. This phenomenon is typical for the microbiology, where the value of minimum inhibitory concentration (MIC) that inhibits the visible growth

of a microorganism after overnight incubation is often used. In our case, the value of MIC lies around 10 % of AgNPs in the PMMA matrix.

Half-inhibition time, which is the time required by bacteria to double their numbers when compared with the start inhibition, was introduced for data presentation. Half-inhibition time of fresh samples and those previously soaked for one week are given in Fig. 7b,c respectively. The inhibition time of the control samples (without silver) is also presented. It is evident that sample preparation procedure does not affect bacterial growth, in the case of silver absence. From Fig. 7b, it is evident that antimicrobial activity of AgNPs/PMMA coating increases with increasing of silver concentration. Differences are more pronounced in the case of AgNPs synthesized at lower temperature. Significantly greater antimicrobial activity show films with 10 % silver concentration and prepared at 75 and 100 °C. On the other hand, samples containing 1 % AgNPs have almost no effect on the growth of bacteria, regardless on the preparation temperature. Similar situation was observed in the case of soaked films. Despite of the some loss of antimicrobial properties, which can be attributed to leaching of unreacted silver ions and AgNPs situated
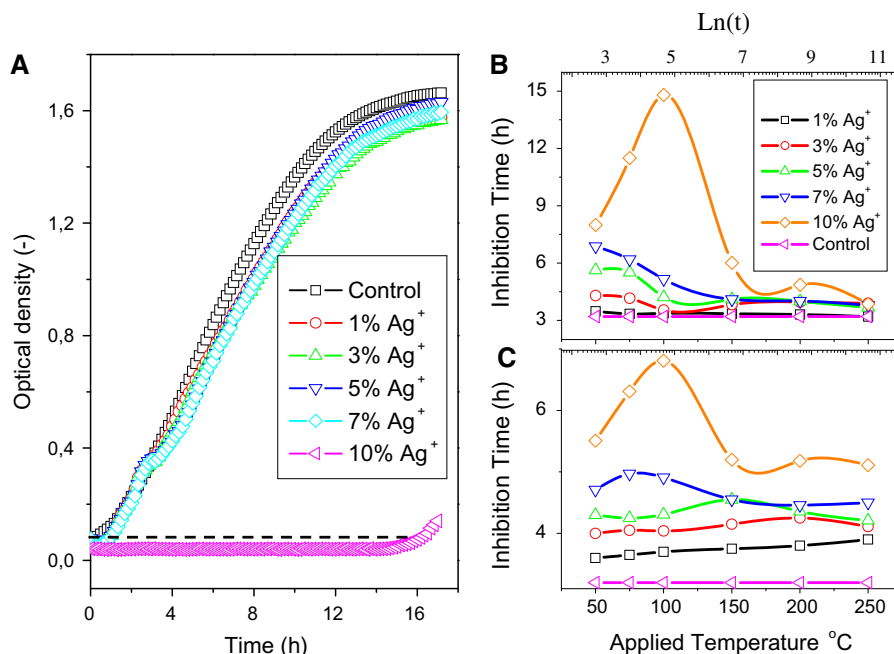

Fig. 7 Dependence of optical density (OD) on the time of bacteria growth in pristine nutrient solution and in nutrient solution with silver extracts added, (**a**) inhibition time of silver extract taken from pristine (**b**) and soaked samples (**c**)

close to sample surface, the samples still exhibit antimicrobial properties. In the case of samples containing 1 % AgNPs, slight increase of antimicrobial activity after soaking was observed. This phenomenon can probably be attributed to the changes of film structure during soaking, which promote more effective release of silver (Lyutakov 2015). Like in the previous case AgNPs/PMMA,films prepared under 75 and 100 °C are most active. Rapid increase of antimicrobial activity after achieving of some critical concentration is not surprising. Antimicrobial activity of silver-containing antimicrobial films strongly depends on silver concentration and usually rapidly increases in some concentration range but remains constant outside (Sanchez-Valdes 2014). However, it is still a question, why only films prepared under 75 and 100 °C are so antimocrobial effective. It is evident that conversion rate cannot explain this phenomenon—there are no significant differences between sample prepared at a temperature of 75 °C or higher. On the other hand, AgNPs/PMMA films prepared at mean conditions have average NPs size between 6 and 6.5 nm and narrower size distribution in comparison with 10 % Ag films prepared at higher temperature. It can, therefore, be concluded that highest antimicrobial activity exhibit films with narrow NPs size distribution around the 6 nm.

Conclusion

New, one-step technique for direct doping of PMMA films with AgNPs was suggested and experimentally verified. Proposed method is environmentally friendly, extremely simple, and fast. The properties of AgNPs/PMMA composite films were examined by different methods and the kinetics of the AgNPs release was studied. Conversion rate of Ag^+ was found to be influenced by both applied temperature and initial Ag ion concentration. NPs shape and distribution depend on the reaction time, applied temperature, and initial silver concentration. Bactericidal properties of AgNPs/PMMA films against Gram-negative bacteria were successfully demonstrated. It was found that antimicrobial activity of prepared films depends on the NPs average size and uniformity. Samples containing 10 % of AgNPs and prepared at 75 and 100 °C showed significantly greater antimicrobial activity comparing to the other samples.

References

Akhter SA, Barry BW (1985) Absorption through human skin of ibuprofen and flurbiprofen; effect of dose variation, deposited drug films, occlusion and the penetration enhancer N-methyl-2-pyrrolidone. J Pharm Pharmacol 37:27–37

Aymonier C et al (2002) Hybrids of silver nanoparticles with amphiphilic hyperbranched macromolecules exhibiting antimicrobial properties. Chem Comm 24:3018–3019. doi:10.1039/B208575E

Behrens S et al (2006) Assembly of nanoparticle ring structures based on protein templates. Adv Mater 18:284–289. doi:10.1002/adma.200501096

Burkowska-But A, Sionkowski G, Walczak M (2014) Influence of stabilizers on the antimicrobial properties of silver nanoparticles introduced into natural water. J Environ Sci 26:542–549. doi:10.1016/S1001-0742(13)60451-9

Cheng YJ et al (2011) In situ formation of silver nanoparticles in photocrosslinking polymers. J Biomed Mater Res, Part B 97B:124–131. doi:10.1002/jbm.b.31793

Cheviron P, Gouanve F, Espuche E (2014) Green synthesis of colloid silver nanoparticles and resulting biodegradable starch/silver nanocomposites. Carbohydr Polym 108:291–298. doi:10.1016/j.carbpol

Chudasama B et al (2010) Highly bacterial resistant silver nanoparticles: synthesis and antibacterial activities. J Nanopart Res 12:1677–1685. doi:10.1007/s11051-009-9845-1

Dallas P, Sharma VK, Zboril R (2011) Silver polymeric nanocomposites as advanced antimicrobial agents: classification, synthetic paths, applications, and perspectives. Adv Coll Interf Sci 166:119–135. doi:10.1016/j.cis.2011.05.008

Damm C, Munstedt H (2008) Kinetic aspects of the silver ion release from antimicrobial polyamide/silver nanocomposites. Appl Phys A 91:479–486. doi:10.1007/s00339-008-4434-1

Fanta GF et al (2013) Preparation of starch-stabilized silver nanoparticles from amylose–sodium palmitate inclusion complexes. Carbohydr Polym 92:260–268. doi:10.1016/j.carbpol.2012.09.016

Fei X et al (2013) Green synthesis of silk fibroin-silver nanoparticle composites with effective antibacterial and biofilm-disrupting properties. Biomacromolecules 14:4483–4488. doi:10.1021/bm4014149

Frolov AI et al (2012) Molecular mechanisms of salt effects on carbon nanotube dispersions in an organic solvent (N-methyl-2-pyrrolidone). Chem Sci 3:541–548. doi:10.1039/C1SC00232E

Giordani S et al (2006) Debundling of single-walled nanotubes by dilution: observation of large populations of individual nanotubes in amide solvent dispersions. J Phys Chem B 110:15708–15718. doi:10.1021/jp0626216

Grubbs RB (2005) Hybrid metal-polymer composites from functional block copolymers. J Polym Sci A 43:4323–4336. doi:10.1002/pola.20946

Ho CH et al (2004) Nanoseparated polymeric networks with multiple antimicrobial properties. Adv Mater 16:957–961. doi:10.1002/adma.200306253

Jain P, Pradeep T (2005) Potential of silver nanoparticle-coated polyurethane foam as an antibacterial water filter. Biotechnol Bioeng 90:59–63. doi:10.1002/bit.20368

Jeon S-H et al (2009) Understanding and controlled growth of silver nanoparticles using oxidized N-methyl-pyrrolidone as a reducing agent. J Phys Chem C 114:36–40. doi:10.1021/jp907757u

Jewrajka SK, Chatterjee U (2006) Block copolymer mediated synthesis of amphiphilic gold-nanoparticles in water and an aqueous tetrahydrofuran medium: an approach for the preparation of polymer–gold nanocomposites. J Polym Sci A 44:1841–1854. doi:10.1002/pola.21293

Jin R-H, Yuan JJ (2005) Fabrication of silver porous frameworks using poly(ethyleneimine) hydrogel as a soft sacrificial template. J Mater Chem 15:4513–4517. doi:10.1039/B507125A

Jou JH, Chang YL, Liu CH (1992) Effects of imide structure/thickness/curing on solvent diffusions in polyimides. Macromolecules 25:5186–5191. doi:10.1021/ma00046a012

Kim MH (2013) Synthesis of silver nanoplates with controlled shapes by reducing silver nitrate with poly(vinyl pyrrolidone) in N-methylpyrrolidone. Cryst Eng Comm 15:4660–4666. doi:10.1039/C3CE40096D

Kong H, Jang J (2008) Antibacterial properties of novel poly (methyl methacrylate) nanofiber containing silver nanoparticles. Langmuir 24:2051–2056. doi:10.1021/la703085e

Kumar R, Münstedt H (2005) Silver ion release from antimicrobial polyamide/silver composites. Biomaterials 26:2081–2088. doi:10.1016/j.biomaterials.2004.05.030

Lim MH, Ast D (2000) Free-standing thin films containing hexagonally organized silver nanocrystals in a polymer matrix. Angew Chem 12:1102–1105

Lyutakov O (2014) Polymethylmethacrylate doped with porphyrin and silver nanoparticles as light-activated antimicrobial material. RSC Adv 4:50624–50630. doi:10.1039/c4ra08385g

Lyutakov O et al (2008) Refractive index of polymethylmethacrylate oriented by fluid temperature under electrical field. J Mater Sci 19:1064–1068. doi:10.1007/s10854-007-9467-2

Lyutakov O et al (2015) Silver release and antimicrobial properties of PMMA films doped with silver ions, nano-particles and complexes. Mater Sci Engin C 49:534–540. doi:10.1016/j.msec.2015.01.022

Manikandan D, Mohan S, Nair KGM (2003) Ag nanocluster functionalized glasses for efficient photonic conversion in light sources, solar cells and flexible screen monitors. Mater Res Bull 38:1545–1550. doi:10.1039/C3NR02798H

Marambio-Jones C, Hoek EM (2010) A review of the antibacterial effects of silver nanomaterials and potential implications for human health and the environment. J Nanopart Res 12:1531–1551. doi:10.1007/s11051-010-9900-y

Melaiye A et al (2005) Silver(I)-imidazole cyclophane gem-diol complexes encapsulated by electrospun tecophilic nanofibers: formation of nanosilver particles and antimicrobial

activity. J Am Chem Soc 127:2285–2291. doi:10.1021/ja040226s

Mie G (1908) Beiträge zur Optik trüber Medien, speziell kolloidaler Metallösungen. Ann Phys 330:377–445. doi:10.1002/andp.19083300302

Mohan YM et al (2006) Fabrication of silver nanoparticles in hydrogel networks. Macromol Rapid Commun 27:1346–1354. doi:10.1002/marc.200600297

Naik RR (2004) Peptide templates for nanoparticle synthesis derived from polymerase chain reaction-driven phage display. Adv Funct Mater 14:25–30. doi:10.1002/adfm.200304501

Phu DV et al (2014) Study on antibacterial activity of silver nanoparticles synthesized by gamma irradiation method using different stabilizers. Nanoscale Res Lett 9:5–9. doi:10.1186/1556-276X-9-162

Qu RJ et al (2014) Preparation and property of polyurethane/nanosilver complex fibers. Appl Surf Sci 294:81–88. doi:10.1016/j.apsusc.2013.11.116

Rai M, Yadav A, Gade A (2009) Silver nanoparticles as a new generation of antimicrobials. Biotechnol Adv 27:76–83. doi:10.1016/j.biotechadv.2008.09.002

Raveendran P, Fu J, Wallen SL (2003) Completely "green" synthesis and stabilization of metal nanoparticles. J Am Chem Soc 125:13940–13941. doi:10.1021/ja029267j

Sanchez-Valdes S (2014) Sonochemical deposition of silver nanoparticles on linear low density polyethylene/cyclo olefin copolymer blend films. Polym Bull 71:1611–1624. doi:10.1007/s00289-014-1144-z

Shameli K et al (2012) Green biosynthesis of silver nanoparticles using Curcuma longa tuber powder. Int J Mol Sci 13:6639–6650. doi:10.2147/IJN.S36786

Sharma VK, Yngard RA, Lin Y (2009) Silver nanoparticles: green synthesis and their antimicrobial activities. Adv Coll Interface Sci 145:83–96. doi:10.1016/j.cis.2008.09.002

Sioss JA, Keating CD (2005) Batch preparation of linear Au and Ag nanoparticle Chains via wet chemistry. Nano Lett 5:1779–1783. doi:10.1021/nl051370u

Son WK, Youk JH, Park WH (2006) Antimicrobial cellulose acetate nanofibers containing silver nanoparticles. Carbohydr Polym 65:430–434. doi:10.1016/j.carbpol.2006.01.037

Sun X et al (2003) One-step synthesis and size control of dendrimer-protected gold nanoparticles: a heat-treatment-based strategy. Macromol Rapid Commun 24:1024–1028. doi:10.1002/marc.200300093

Svorcik V, Lyutakov O, Huttel I (2008) Thickness dependence of refractive index and optical gap of PMMA layers prepared under electrical field. J Mater Sci 19:363–367. doi:10.1007/s10854-007-9344-z

Vukoje ID et al (2014) Characterization of silver/polystyrene nanocomposites prepared by in situ bulk radical polymerization. Mater Res Bull 49:434–439. doi:10.1016/j.materresbull.2013.09.029

Washio I et al (2006) Reduction by the end groups of poly(vinyl pyrrolidone): a new and versatile route to the kinetically controlled synthesis of Ag triangular nanoplates. Adv Mater 18:1745–1749. doi:10.1002/adma.200600675

Yoksan R, Chirachanchai S (2009) Silver nanoparticles dispersing in chitosan solution: preparation by gamma-

rayirradiation and their antimicrobial activities. Mater Chem Phys 115:296–302. doi:10.1016/j.matchemphys

Zellers ET, Sulewski R (1993) ASTM F739 method for testing the permeation resistance of protective clothing materials: critical analysis with proposed changes in procedure and test cell design. Am Ind Hyg Assoc J 54:465–479. doi:10.1202/0002-8894